Title or Subject: Dynamic Photoelastic Investigation of Crack Arrest

Type of Document of Subtitle and Date:

Montly Progress Report for March 1978

Author(s) and Affiliation:

T. Kobayashi
University of Maryland
College Park, Maryland 20742

NRC Individual to Whom Inquiries Should be Addressed:

C. Z. Serpan
Division of Reactor Safety Research
Office of Nuclear Regulatory Research

This document contains preliminary data
or information subject to change.

U. S. Nuclear Regulatory Commission
Washington, D. C. 20555

Re Contract No. NRC-04-76-172

Monthly Progress Report for March 1978

A Dynamic Photoelastic Investigation of Crack Arrest

I. Accomplishments to Date

A-Z Accomplishments as listed in the December 1977 Progress Report

1. Completed tests on monolithic and duplex ring tests to study steady-state thermal stress effect on crack behavior.
2. Completed investigation of MRL procedure for K_{I_a} determination using polymeric models of tentative standard test specimen.
3. Examined BCL Procedures using the one-dimensional BCL computer code and polymeric models of tentative standard test specimens.
4. Completed initial development of 2D dynamic code.

II. Progress during the Month of February

1. Discussed the BCL reference curve dependence on the shapes of å vs. K relationship with Dr. P. Gehlen of BCL.

   The results of Dr. Gehlen's computation with the BCL code with the University of Maryland å vs. K relationship are tabulated in Table 1 and also shown in Figures 1 and 2.

Table 1

K_Q	$\Delta a/a_o$	K_D/K_Q	V/C_o
0.5	0.33	0.80	0.067
0.6	0.77	0.67	0.088
0.7	1.34	0.57	0.12
0.8	1.70	0.50	0.12

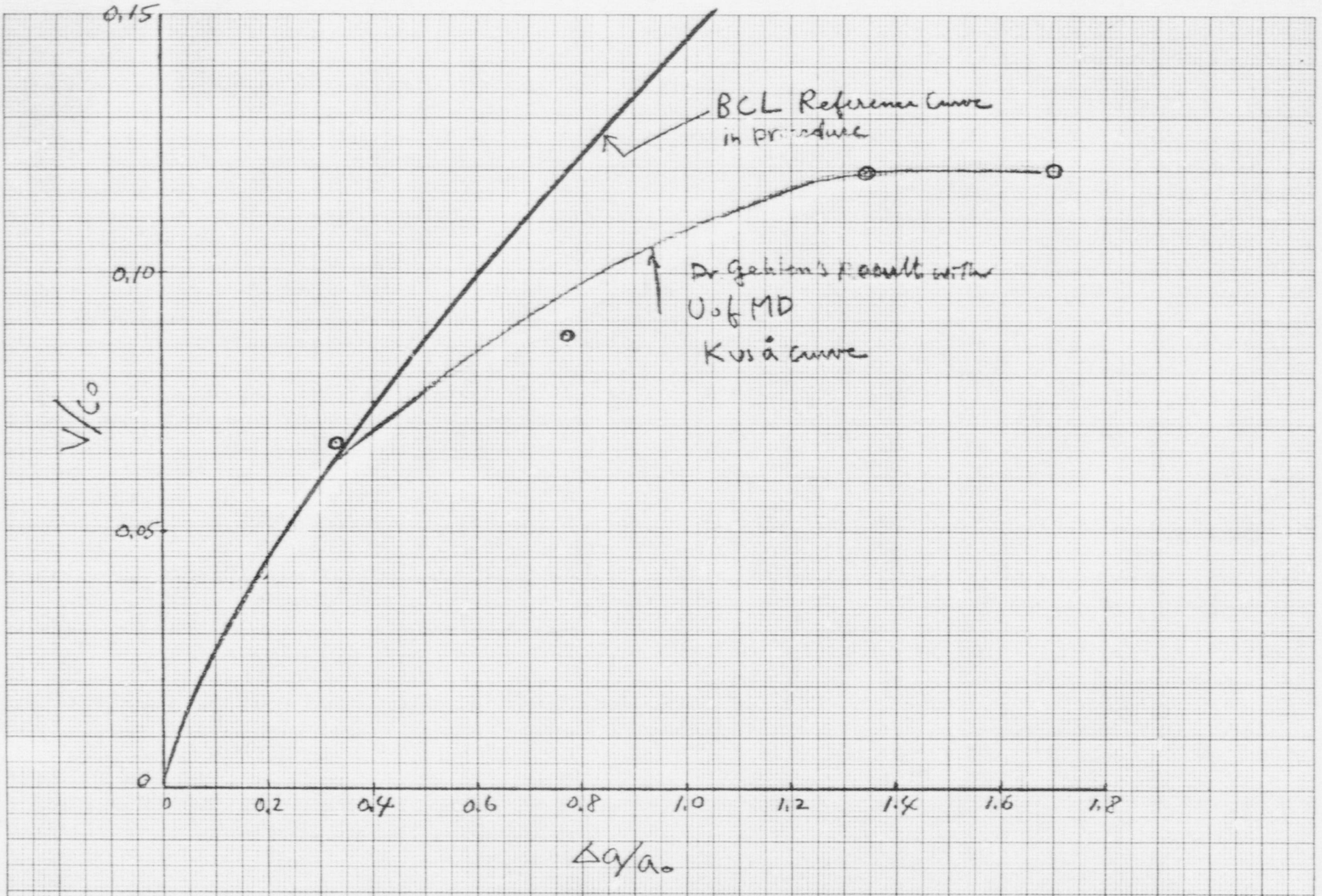

Fig. 1 Velocity Reference Curve with the Univ. of MD K vs à Curve

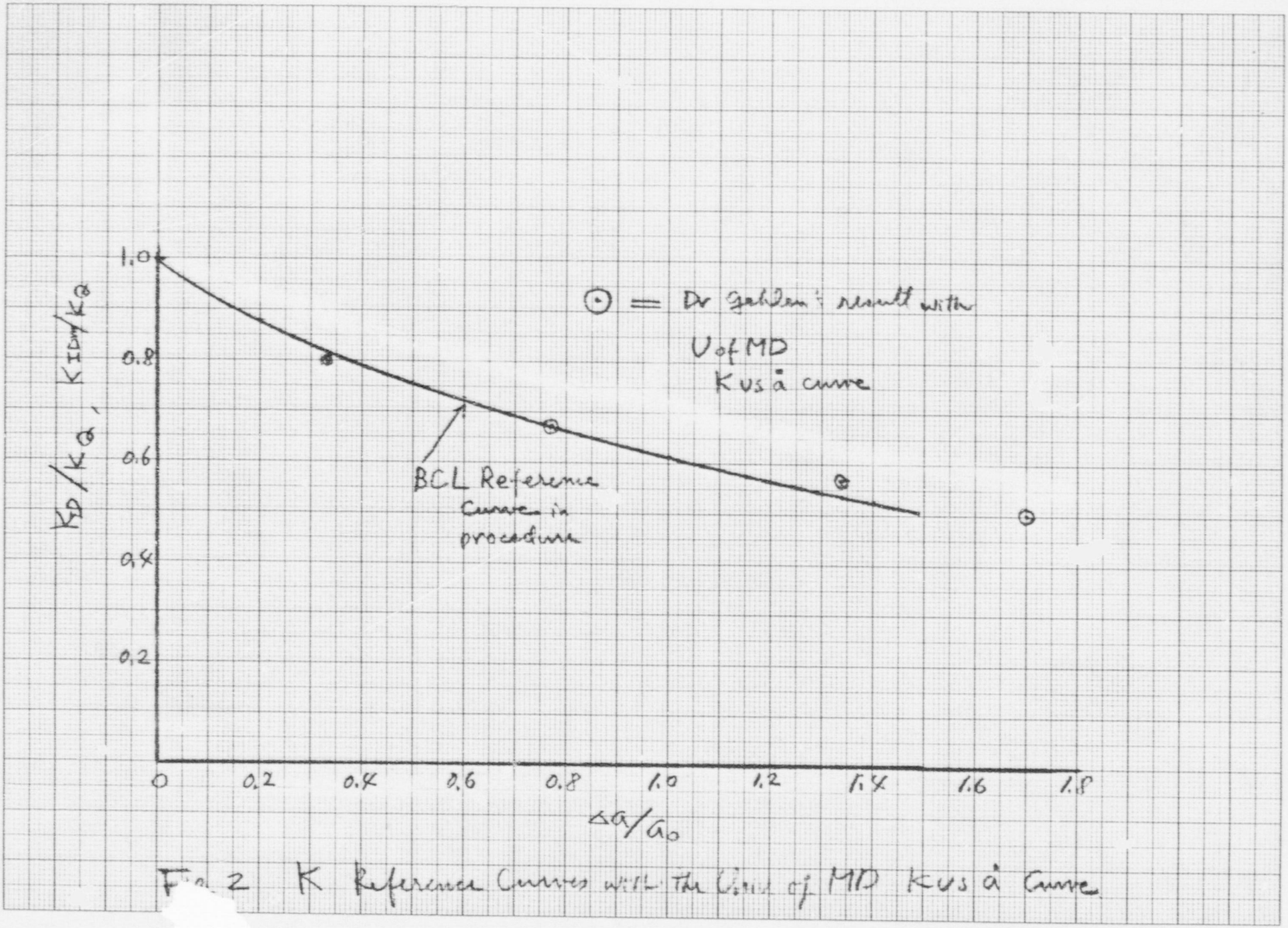

Fig. 2 K Reference Curves with the Use of MD K vs à Curve

2. Further investigation of the dynamic correction for the K determination.

   A short report on the subject is prepared by Dr. H. P. Rossmanith and Dr. G. R. Irwin and is attached to this progress report.

3. Run three birefringent coated 4340 steel

   In two specimens a crack arrest was not observed. In the third specimen a crack arrest was observed approximately 30 mm away from the back end of the specimen. In all three cases isochromatic fringe loops were photographed successfully.

4. Performed static characterization of face-grooved compact specimen. Objective is two-fold: (1) Examination of fringe loops size to K relationship for face-grooved specimen, (2) Establishment of G vs. a for static case.

5. Modified 2D code for constant displacement test.

III. Plans for April

1. Continue test with birefringent coated 4340 steel for characterization of crack arrest.

2. Continue test with face-groove compact specimen.

3. Instrumentation of ring specimen loading fixture for measurement of load.

4. Continue characterization of crack behavior in ASTM crack arrest compact specimen with 2D code.

The Dynamic Correction for the K - Determination

(prepared for the U. S. Nuclear Regulatory Commission, March, 1978)

by

H. P. Rossmanith and G. R. Irwin

Abstract

This work is concerned with the method for determining dynamic stress intensity factors K from photoelastic isochromatic fringes. The primary objective is to illustrate the differences in the K-values obtained from static and dynamic analysis. Statistics is employed to study the correlation between deviations in experimental measurements and the K-value. Implications of the dynamic correction of K onto the K vs $\dot{a}$ - curve are explained. Finally, the accuracy of both methods for determining K, the photoelastic approach and the shadow optical caustic method is inspected within the framework of statistics.

Introduction

Post and Wells [1] were the first to apply photoelastic methods to fracture mechanics in the early 1950's. Irwin [2] in a discussion to Ref. 1 showed that the stress-intensity factor K could be determined from a single isochromatic fringe loop at the tip of the crack. According to Irwin's method the stress intensity factor K and a uniform stress field σ_{ox} are functions of the radius r_m of the fringe loop and its angle of tilt θ_m as defined in Fig 1.

Several authors, e.g. Bradley and Kobayashi [3] have modified Irwin's method. But the common feature of all approaches is the appearance of only two basic quantities, K and σ_{ox}. All these two-parameter methods of fracture analysis for the determination of the stress intensity factor from photoelastic isochromatic fringe data have been critically reviewed recently by Etheridge and Dally [4]. These authors investigated and compared the range of applicability of the diverse methods and computed error bounds for the two-parameter solutions.

Employing the results of Irwin's analysis of the constant velocity semi-infinite tensile crack opened by a traveling line force the stress field for the constant speed moving crack may be derived. The results obtained can be modified to give a so-called three parameter solution where

a second order term has been added in the stress field representation.

This third parameter, β, is kept arbitrary to match the shape of the fringe loop; Physically, β counts for variations in the remote stress field and the finiteness of the specimen investigated.

Etheridge [5] compared the two- and three-parameter dynamic solution to the corresponding two- and three-parameter static solutions, respectively, introduced several geometrical approximate relations which simplified the analysis and prove the convergence of the dynamic solution to the static solution. The comparison between static and dynamic results then showed that the static solution overestimates the K-value by 5.76% at the high velocity of 16,700"/sec. This was supported by the strong similarity between the computer-generated static and dynamic fringe loops which showed practically no difference.

The use of the exact formulae, however, reveals appreciable differences between the static and dynamic K-value for moderate and high crack propagation velocities. The results exhibit smaller K-values for the dynamic case and the difference between static and dynamic K-value exceeds the 5% deviation line in almost all cases.

In the following the corrected dynamic stress-intensity factor K vs tilt angle θ_m curves as a function of the crack velocity are presented. Statistical correlation theory is employed to study the influence of variations in the measured quantities θ_m and r_m onto the K-factor.

Analysis

Utilizing the same terminology and notation as in Ref. [5] the results of all two- and three-parameter methods may be reduced to the fundamental equation

$$\frac{K}{2\bar{c}m\sqrt{2\pi r_m}} = H(\theta_m, \beta \frac{r_m}{a}) \qquad (1)$$

where a is a length factor constant which can be selected to equal crack size, r_m for a particular isochromatic fringe loop, etc. The parameter α involving σ_{ox} ($\alpha = \sigma_{ox}\sqrt{2\pi r_m}/K$) is not included in eq.(1) because it can be found using the conditions for $\theta = \theta_m$. The maximum shear stress, $\bar{\tau}m$, is given by

$$\tau_m = \frac{Nf_\sigma}{2h} \tag{2}$$

Here, r_m and θ_m are the maximum radius and the tilt angle of the fringe loop, respectively, N is the fringe order, h is the specimen thickness, and f is the dynamic stress optic constant.

For the two-parameter method, where $\beta = 0$, the equation (1) takes the form

$$\frac{K}{2\tau_m\sqrt{2\pi r_m}} = H(\theta_m) \tag{3}$$

where $H(\theta_m)$ is an implicit function of the crack velocity $\dot{a}$ but is independent of r_m.

The normalized stress parameter $\sigma_{ox}/2\tau_m$ is given by

$$\frac{\sigma_{ox}}{2\tau_m} = F(\theta_m, \beta\frac{r_m}{a}) \tag{4}$$

for the three-parameter method and by

$$\frac{\sigma_{ox}}{2\tau_m} = F(\theta_m) \tag{5}$$

for the two-parameter method.

Results and Discussion

Results for the normalized stress intensity factor $K/2\tau_m\sqrt{2\pi r_m}$ obtained from eq.(3) are shown in Fig 2 as a function of θ_m over the experimentally observed range of $70 < \theta_m < 130$ degress. Different curves correspond to different crack velocities. The curve "0" represents the static crack whereas "4" represents a very high velocity propagating crack. Usually, the crack velocity $\dot{a}$ = 9000 "/sec for low velocity propagating cracks and $\dot{a}$ = 15,000 "/sec for high velocity cracks. The curves K vs θ_m are shape-invariant over a large region of crack velocities and the value of θ_m correlated to the maximum K-value for a given $\dot{a}$ shifts slightly from 110° to 115° when $\dot{a}$ increases from 0 to 16,000 "/sec.

Low crack velocity $\dot{a}$ 9000 "/sec $\hat{=}$ 229 m/s

The difference between static and dynamic stress-intensity factor for different velocities is depicted in Fig 3. The curve "1" representing low crack propagation traces within the 5% error bound for tilt angles $82° < \theta_m < 130°$. These angles correspond to backward leaning loops and slightly forward leaning loops. Such loop tilts are mostly recorded for DCB-specimens. Thus, for these specimens, the static analysis provides acceptable results for low velocity crack propagation.

High crack velocity 9000 "/sec $< \dot{a} <$ 16,000 "/sec

In this case, the differences in K between static and dynamic analysis are by far too large and the static analysis gives too high values for K. All K vs θ_m-curves lie outside the 5% error range! The minimum error $(K_{stat} - K_{dyn})/ K_{stat}$ for $\dot{a}$ = 12,000 "/sec is 7% (at $\theta_m = 107°$) and it is 12% for $\dot{a}$ = 16,000 "/sec (at $\theta_m = 109°$). Notice, that the minimum error for very high crack velocity $\dot{a}$ = 24,000 "/sec is 28%!

For backward leaning loops (DCB-specimens) the relative error varies only slightly as a function of θ_m ($95° < \theta_m < 115°$). The differences in K become again larger for very strongly backward leaning loops. The relative error increases gradually with decreasing tilt angle within an intermediate range of θ_m ($85° < \theta_m < 95°$), where the loops are nearly standing straight up.

However, the discrepancy between dynamic and static solution becomes increasingly severe for decreasing θ_m, i.e. for forward leaning loops encountered with SEN-specimens. Here, the relative error increases almost exponentially and the dynamic correction of K is inevitable.

Similarly, results for the normalized stress parameter $\sigma_{ox}/2\tau_m$ and $\sigma_{ox}\sqrt{2\pi r_m}/K$ obtained from eqs. (3) and (5) are shown in Fig 4a, b, as a function of the tile angle θ_m for various crack velocities. Notice, the remarkable trend of the zero-crossings to shift towards higher values of θ_m (90° in the static case → 96° for high velocity crack).

$\dot{a}$ vs K-characterization for Homalite 100

In the past experimental data in conjunction with the static K-analysis were used to determine the $\dot{a}$ vs K-relationship for Homalite 100 for a variety of different types of specimens (SEN, R-DCB, C-DCB,...)[6]. This Γ-shaped curve which is assumed to be a material invariant is shown in Fig 5.

In the stem of the curve crack velocity changes are very large ($0 \leq \dot{a} <$ 9000 "/sec) with extremely small changes in K near its arrest value. Here, changes introduced by the dynamic correction are minor; thus, this portion of the curve remains almost unchanged. In the intermediate range at velocities of 10,000 - 12,000 "/sec the $\dot{a}$ vs K curve changes slope appreciably. The dynamic correction works against this trend by increasing the slope and shifting the curve towards lower K-values.

The upper part of the $\dot{a}$ vs K-curve, the so-called "second plateau" where even large changes in K produce small $\dot{a}$-changes only alters appreciably. The dynamic correction does not change the altitude of the plateau, however, it shifts points on the plateau to the left, i.e. to considerably lower K-values. This implies that unsuccessful attempt to and succesful crack branching occur at lower K-values than assumed in the past [7]. This structural change of the $\dot{a}$ vs K curve for two different specimens is illustrated in Fig 6. The SEN-sample exhibiting forward leaning loops is extremely sensitive to the dynamic correction, whereas the R-DCB-specimen possessing backward leaning loops is almost insensitive to dynamic corrections. Fig 7 shows the relationship between the $\dot{a}$ vs K-curve and the adjoint σ_{ox}-values for different types of specimens.

Employing the relation between the dynamic strain energy release rate G_v and crack velocity [8]

$$G_v = \frac{1-\nu^2}{E} K_v^2 A(v) \qquad (6)$$

where K_v is the dynamic stress intensity factor and A(v) is a velocity correction the $\dot{a}$ vs G-curve may be constructed.

Error Analysis for K-Determination

The primary objective of this chapter is the study of the influences of irevitable experimental errors in the θ_m, and r_m measurements onto the K-value determination. Given the spread of measurements in the graphical determination of θ_m and r_m from photographically recorded isochromatic fringe patterns the mean and the deviation of K may be computed by means of methods of statistical correlation theory. Moreover, if statistics is

applied in the same way to the shadow optical method of K-determination (IFKM, Freiburg, West Germany) and the results are compared with the results from photoelasticity a first step towards the decision which method should be given the preference is possible. Table I summarizes the analytical expressions.

Fig 8 shows the normalized deviation $\sigma_{K_{ph}}/\sigma_{\theta_m}$ vs tilt angle θ_m. Since the normalized deviation is directly proportional to the slope of the $\dot{a}$ vs K-curve it is zero at the maximum value of K for $\theta_m = 110°$ and it increases considerably for forward leaning loops (SEN-specimen). The difference between static and dynamic deviation is negligible.

The ratio

$$\frac{\sigma_{K_{ph}}}{\sigma_{K_c}} = \frac{\dot{K}_{ph}}{K'_c} \quad \frac{\sigma_{\theta_m}}{\sigma_D} = \Psi(K, \theta_m, D) \qquad (7)$$

is a function of the tilt angle and the caustic diameter D. Whenever the ratio $\sigma_{K_{ph}}/\sigma_{K_c}$ exceeds the value 1 the method of caustics is more reliable to determine K than the method of photoelasticity.

Work in Progress

Current and future work is directed towards improvement of the K-determination and comparison of the reliability of both methods photoelasticy and the method of caustic. Several distinct problems will be investigated:

1) Influence of higher order terms in the Westergaard function (α,β) cnto the accuracy of the K-determination.
2) Distribution of σ_{ox}-values and selection of a possible structure of this distribution with respect to (experimental data points in) the $\dot{a}$ vs K-curve.
3) Development of a dynamic two-loop method for the K-determination from two arbitrary isochromatic fringe loops.
4) Comparative study of the reliability and accuracy of the photoelastic method and the method of caustics within the framework of statistical error analysis.

References

1. Wells, A., Post, D., "The dynamic stress distribution surrounding a running crack - a photoelastic analysis", Proc. SESA 11, 69-92, 1958.

2. Irwin, G. R., Discussion of Ref. 1, Proc. SESA 16, 93-96, 1958.

3. Bradley, W. B., Kobayashi, . A., "An investigation of propagating cracks by dynamic photoelasticity", Exp. Mech. 10, 106-113, 1970.

4. Etheridge, J. M., Dally, J. W., "A critical review of methods for determining stress intensity factors from isochromatic fringes", Exp Mech. 17, 248-254, 1977.

5. Irwin, G. R., et.al., "A photoelastic characterization of dynamic fracture", U.S. NRC-Report NUREG-0072, Univ. of Maryland, 1976.

6. Irwin, G. R., et.al, "A photoelastic study of the dynamic fracture behavior of Homalite 100, U. S. NRC-Report NUREG-75-107, Univ. of Maryland, 1975.

7. Etheridge, J. M., Dally J. W., Kobayashi, T., "A new method of determining the stress intensity factor K from isochromatic fringe loops", Eng. Fract. Mech. 10, 81-93, 1978.

8. Freund, L. B., "Crack propagation in an elastic solid subjected to general loading - I. Constant rate of extension", J. Mech. Phys. Solids 20, 129-140, 1972.

Table I Comparative statistical study of photoelasti. method and caustic method for K-determination

Error Source	Caustic	Photoelasticity
Geometry	D, Z_o, L	θ_m, r_m
Material	f_c, f_i, ν, E	ν, E, ρ, f_σ

Stress Intensity Factor

$$K_c = \frac{2\sqrt{2\pi}\, E\, \ell^{3/2}}{3\, f_{\sigma,i}^{5/2}\, \nu\, d} \frac{D^{5/2}}{L^{3/2} Z_o} = \beta_c\, H_c(D)$$

$$K_{ph} = \frac{N f_\sigma}{d} \sqrt{2\pi r_m}\; H(\theta_m) = \beta_{ph}\, H_{ph}(\theta_m)$$

Expected Value $$E\{\underline{K}_c\} \doteq K_c \left\{1 + \frac{15}{8} \frac{\sigma_D^2}{D^2}\right\}$$

$$E\{\underline{K}_{ph}\} \doteq K_{ph} \left\{1 + \frac{1}{2} \frac{\ddot{H}}{H} \sigma_{\theta_m}^2\right\}$$

Deviation $$\sigma_{K_c} = K_c'\, \sigma_D$$

$$\sigma_{K_{ph}} = \dot{K}_{ph}\, \sigma_{\theta_m}$$

$$(\,)' = \frac{\partial}{\partial D}, \quad (\,)^{\cdot} = \frac{\partial(\,)}{\partial \theta_m}$$

Table 2 Normalized stress parameters $\sigma_{ox}/2\tau_m$ and $\sigma_{ox}\sqrt{2\pi r_m}/K$ vs tilt angle θ_m for various crack velocities $\dot{a}$

Static Case

θ_m	$\sigma_{ox}/2\tau_m$	$\sigma_{ox}\sqrt{2\pi r_m}/K$
72	0.6851	2.0002
75	0.4595	0.7928
80	0.2335	0.2907
85	0.0956	0.1033
90	0.0	0.0
95	-0.0734	-0.0701
100	-0.1348	-0.1252
105	-0.1903	-0.1739
110	-0.2441	-0.2216
115	-0.2994	-0.2729
120	-0.3592	-0.3333
125	-0.4266	-0.4109

$\dot{a}$ = 9000 in/sec

θ_m	$\sigma_{ox}/2\tau_m$	$\sigma_{ox}\sqrt{2\pi r_m}/K$
72	0.7370	2.598
75	0.5030	0.9537
80	0.2697	0.3571
85	0.1273	0.1446
90	0.0279	0.0271
95	-0.0489	-0.0497
100	-0.1137	-0.1085
105	-0.1727	-0.1627
110	-0.2301	-0.2169
115	-0.2892	-0.2757
120	-0.3531	-0.3435
125	-0.4250	-0.4294

$\dot{a}$ = 16000 in/sec

θ_m	$\sigma_{ox}/2\tau_m$	$\sigma_{ox}\sqrt{2\pi r_m}/K$
72	0.8497	5.3522
75	0.5975	1.4300
80	0.3491	0.5311
85	0.1973	0.2507
90	0.0901	0.1038
95	0.0057	0.0059
100	-0.0069	-0.00712
105	-0.1341	-0.1394
110	-0.2022	-0.2062
115	-0.2686	-0.2789
120	-0.3424	-0.3649
125	-0.4249	-0.6423

Table 3 The distribution of σ_{ox} in the $\dot{a}$ vs K relationship

EPL-Test No. 9 & 10 (NRC I)

Fringe order	r_{max}	θ_{max}	$\dot{a}$	K_{stat}	K_{dyn}	σ_{ox}
1	2.13	80	14700	875.9	740.6	98.634
2	0.49	85	14700	968.7	845.6	107.984
1	1.40	94	14000	918.9	829.6	0.546
2	0.30	94	14000	850.7	768.1	1.091
1	0.75	92	13400	660.9	600.5	8.402
2	0.18	92	13400	647.6	588.4	16.804
1	0.38	99	11200	493.9	464.7	-26.614
2	0.30	111	10800	450.8	426.7	-70.324
1	0.24	116	9000	400.6	385.3	-89.891
1	0.21	121	6200	366.9	359.8	-110.132

CLL-Test 21 - 3/8"

Fringe order	r_{max}	θ_{max}	$\dot{a}$	K_{stat}	K_{dyn}	σ_{ox}
1	0.33	79	5500	330.2	322.6	84.44
2	0.08	89	5500	417.6	410.8	16.41
1	0.35	77	4900	303.8	297.3	108.87
2	0.08	87	4900	405.8	400.3	37.34
1	0.31	80	2900	334.2	332.2	70.73
2	0.08	85	2900	391.4	389.5	58.98
1	0.33	83	2300	379.7	378.5	43.57
2	0.08	85	2300	391.4	390.2	58.25
1	0.30	85	2000	379.0	378.1	28.98
2	0.08	86	2000	298.9	397.9	45.05
1	0.31	87	1200	399.4	399.1	16.20
2	0.08	87	1200	405.8	405.5	32.41
1	0.32	89	1100	417.6	417.2	5.15
2	0.08	88	1100	411.9	411.6	20.97
Dimensions	[in]	[degrees]	[in/sec]	[psi$\sqrt{in}$]	[psi$\sqrt{in}$]	[psi]

Fig 1 Characteristic geometry of the isochromatic fringe loop at the crack tip.

Fig 2 Normalized stress intensity factor $K/2\tau_m\sqrt{2\pi r_m}$ as a function of tilt angle θ_m for various crack velocities $\dot{a}$.

Fig 3 Relative error as a function of tilt angle θ_m for various crack velocities $\dot{a}$.

Fig 4a Normalized stress parameter $\sigma_{ox}/2\tau_m$ as a function of tilt angle θ_m for various crack velocities $\dot{a}$.

Fig 4b (= Table 2) Normalized stress parameter $\sigma_{ox}\sqrt{2\pi r_m}/K$ vs tilt angle θ_m for various crack velocities $\dot{a}$.

Fig 5 Crack velocity $\dot{a}$ vs stress intensity factor K for Homalite 100.

Fig 6 Crack velocity $\dot{a}$ vs stress intensity factor K for Homalite 100 determined with SEN specimens.

Fig 7 (= Table 3) The distribution of σ_{ox} in the $\dot{a}$ vs K relationship.

Fig 8 Normalized deviation Δ vs tilt angle θ_m for static and high speed crack.

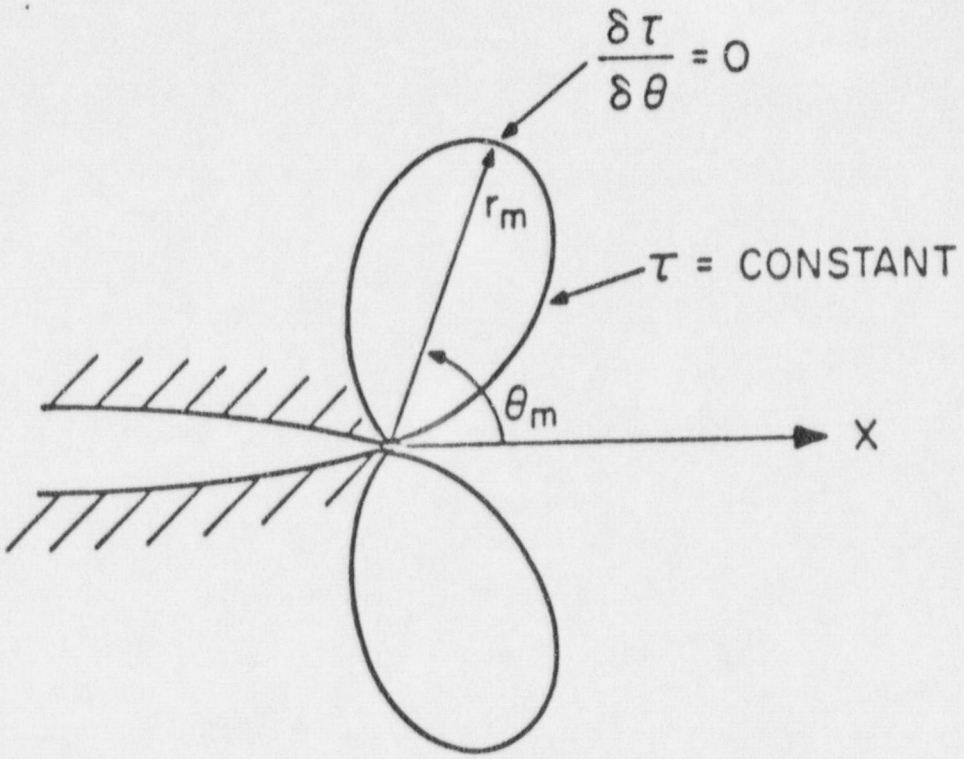

Fig 1 Definition of r_m and θ_m Associated with an Isochromatic Fringe Loop

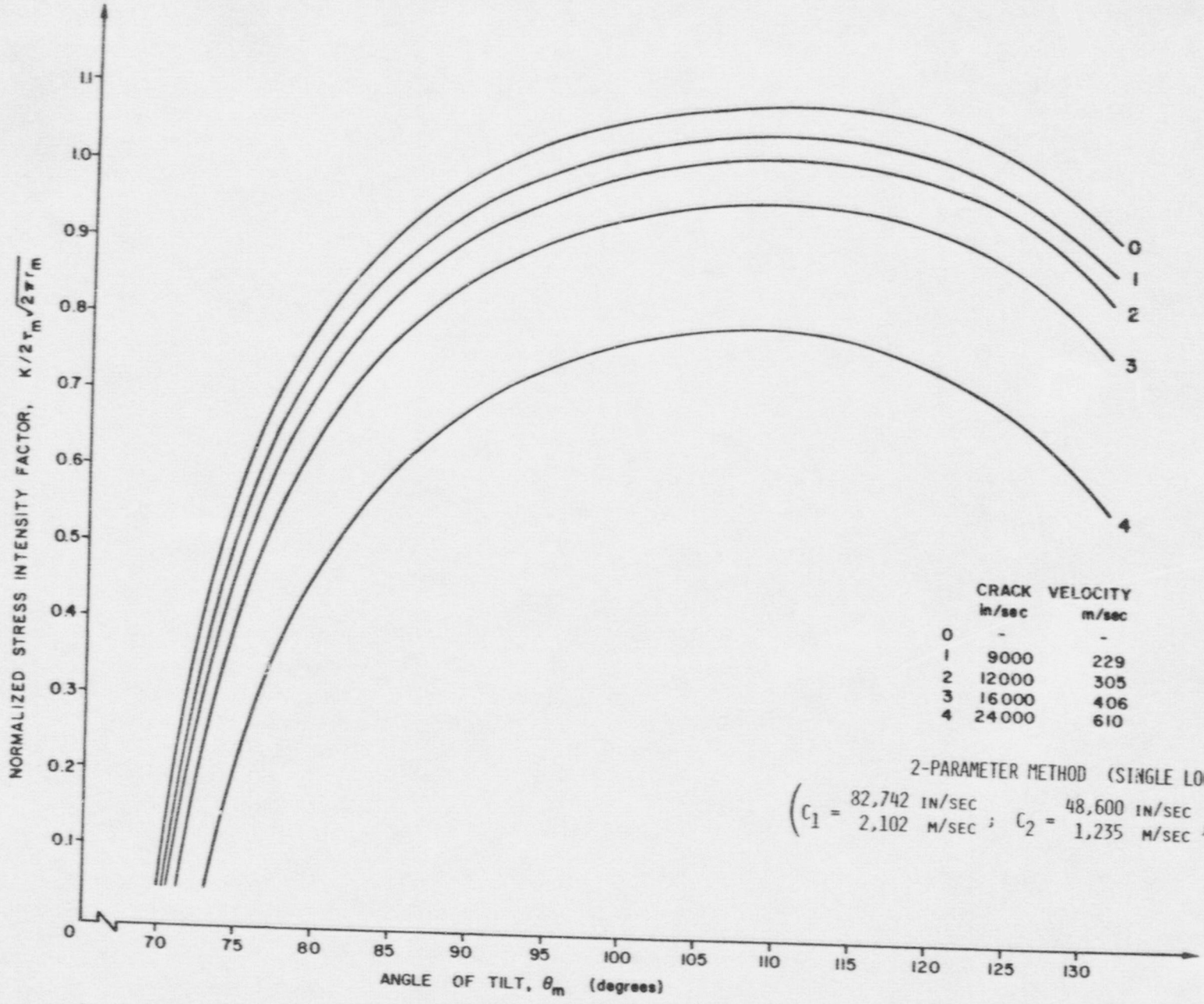

	CRACK VELOCITY in/sec	m/sec
0	-	-
1	9000	229
2	12000	305
3	16000	406
4	24000	610

2-PARAMETER METHOD (SINGLE LOOP)

$\left(C_1 = \begin{matrix} 82{,}742 \text{ IN/SEC} \\ 2{,}102 \text{ M/SEC} \end{matrix} ; \quad C_2 = \begin{matrix} 48{,}600 \text{ IN/SEC} \\ 1{,}235 \text{ M/SEC} \end{matrix} ; \quad \nu = 0.31\right)$

2-PARAMETER METHOD (SINGLE LOOP)

$\left(C_1 = \begin{matrix} 82{,}742 \text{ IN/SEC} \\ 2{,}102 \text{ M/SEC} \end{matrix} ; C_2 = \begin{matrix} 48{,}600 \text{ IN/SEC} \\ 1{,}235 \text{ M/SEC} \end{matrix} ; \nu = 0.31\right)$

	CRACK VELOCITY	
	in/sec	m/sec
1	9000	229
2	12000	305
3	16000	406
4	24000	610

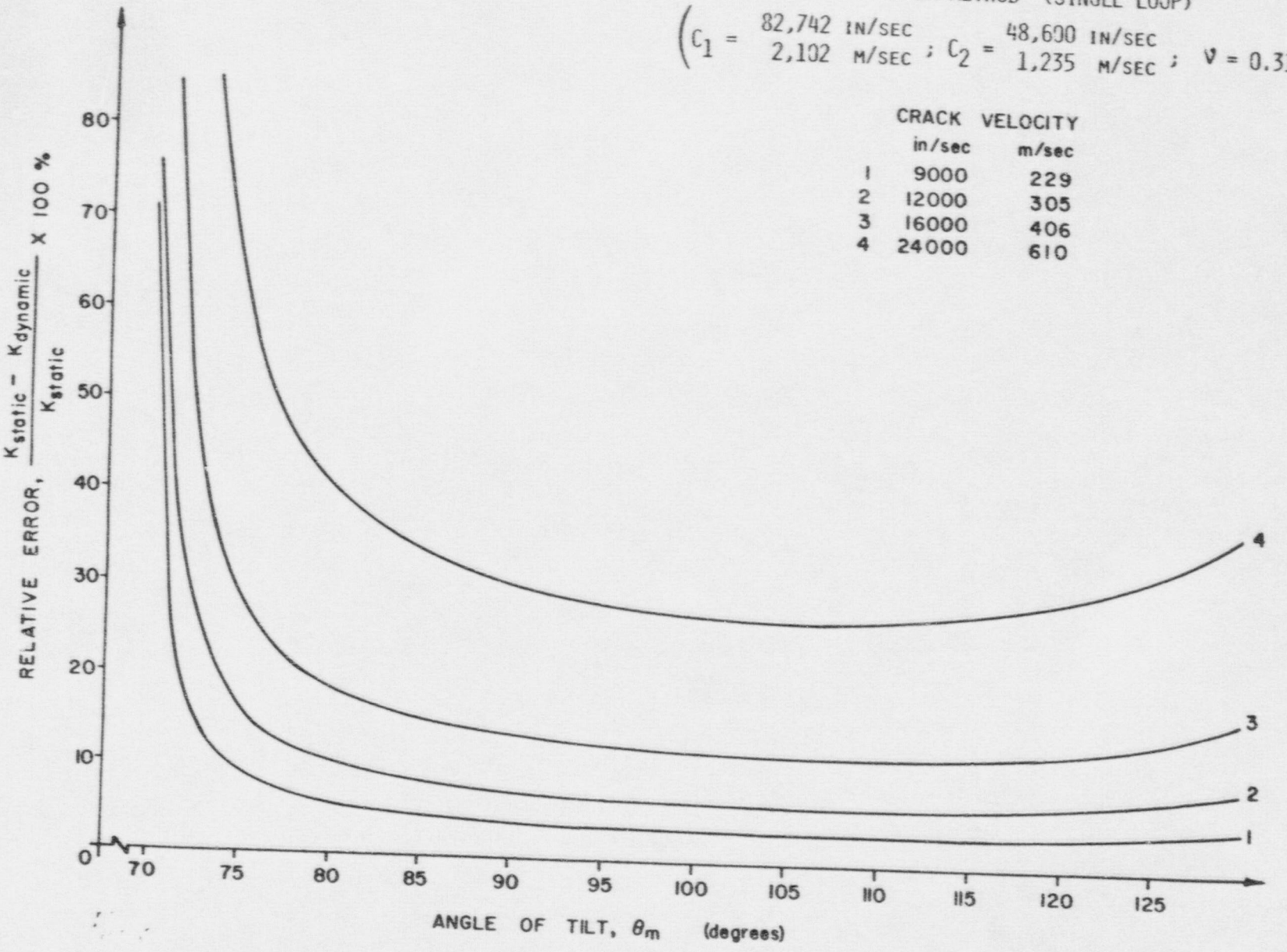

2-PARAMETER METHOD (SINGLE LOOP)

$\left(C_1 = \begin{matrix} 82{,}742 \text{ IN/SEC} \\ 2{,}102 \text{ M/SEC} \end{matrix} ; C_2 = \begin{matrix} 48{,}600 \text{ IN/SEC} \\ 1{,}235 \text{ M/SEC} \end{matrix} ; \quad \nu = 0.31\right)$

	CRACK VELOCITY	
	in/sec	m/sec
0	-	-
1	9000	229
2	12000	305
3	16000	406
4	24000	610

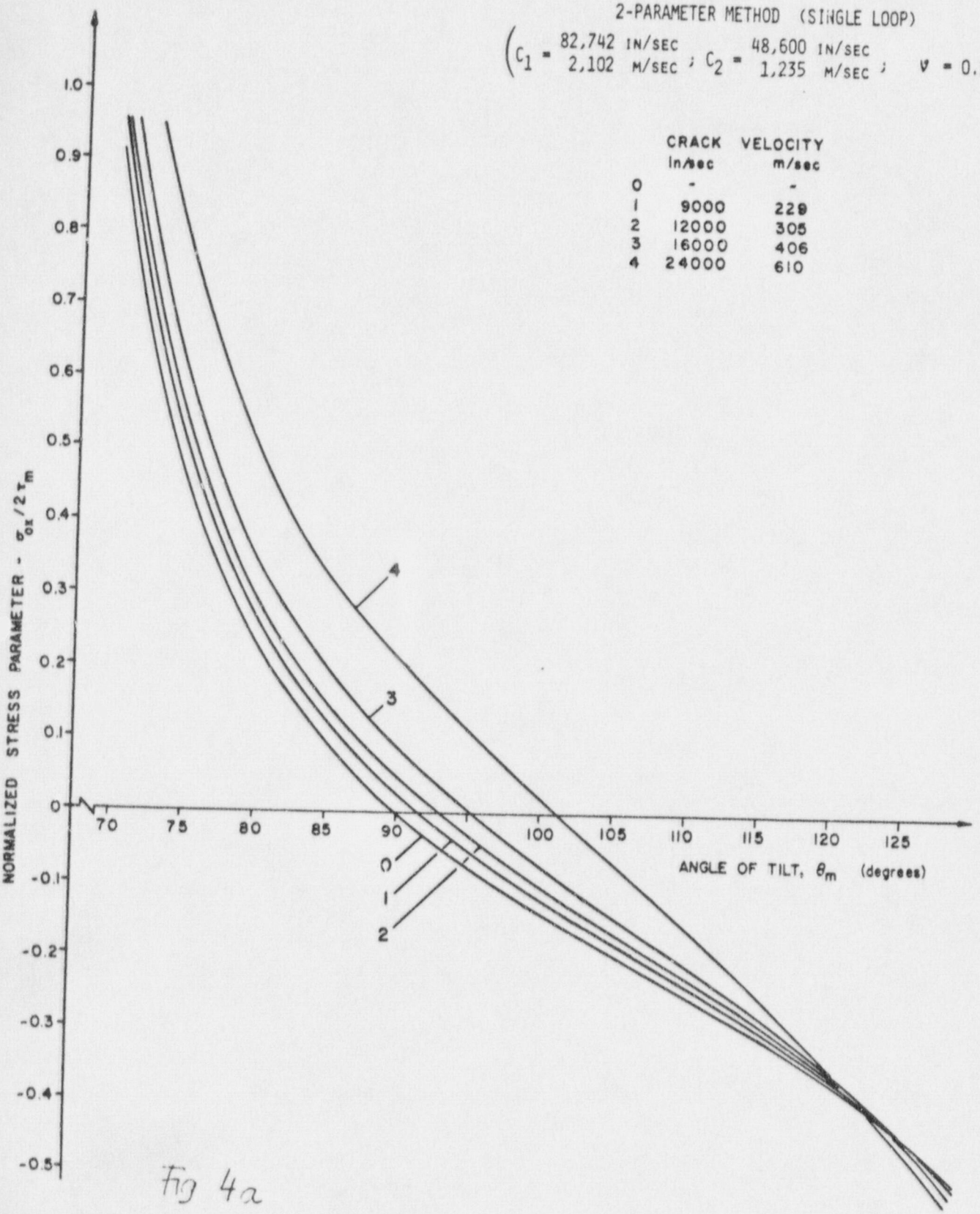

Fig 4a

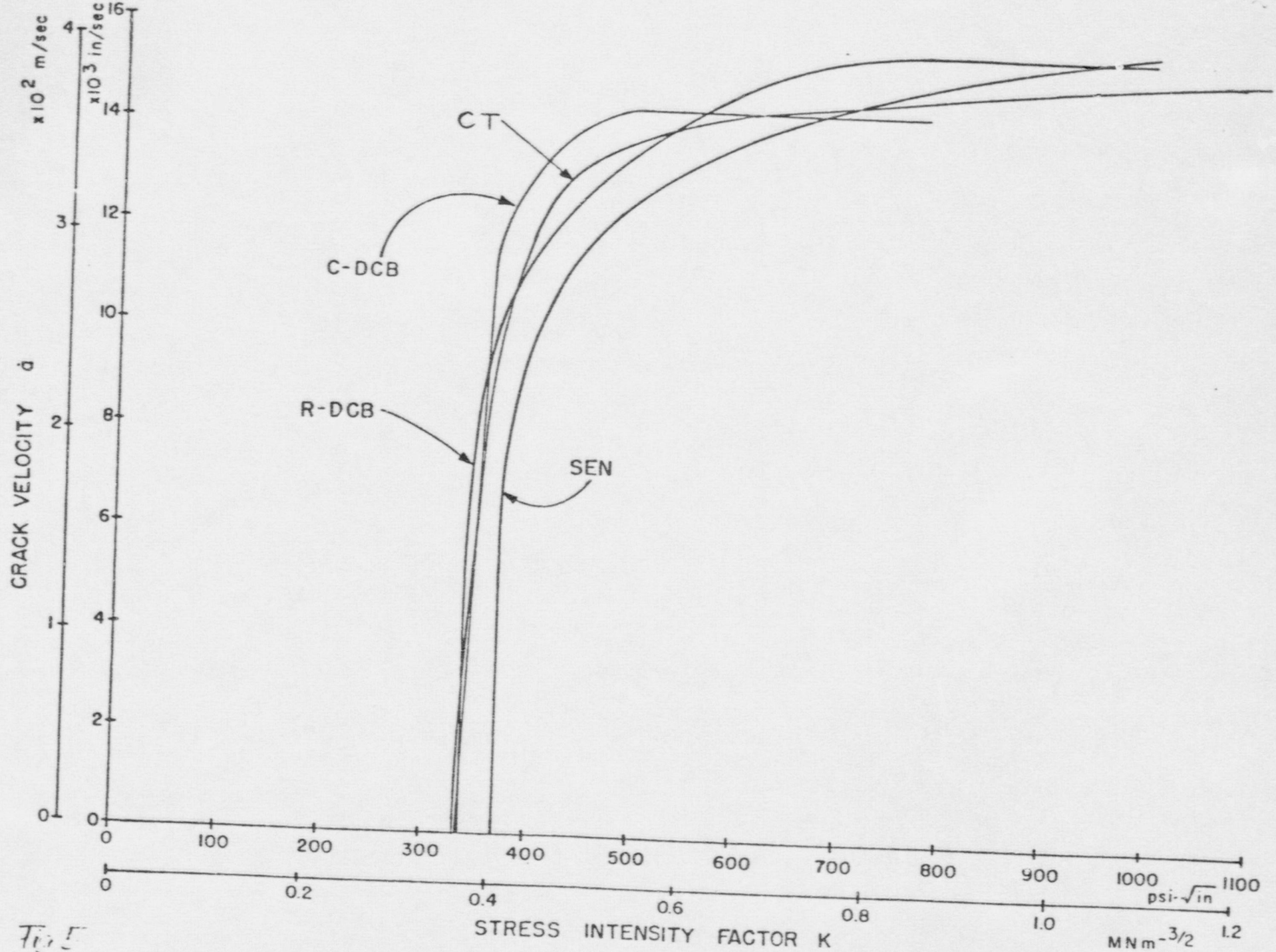
CRACK VELOCITY ȧ
x10² m/sec
x10³ in/sec
CT
C-DCB
R-DCB
SEN
STRESS INTENSITY FACTOR K
psi-√in
MNm⁻³/²

Fig 5

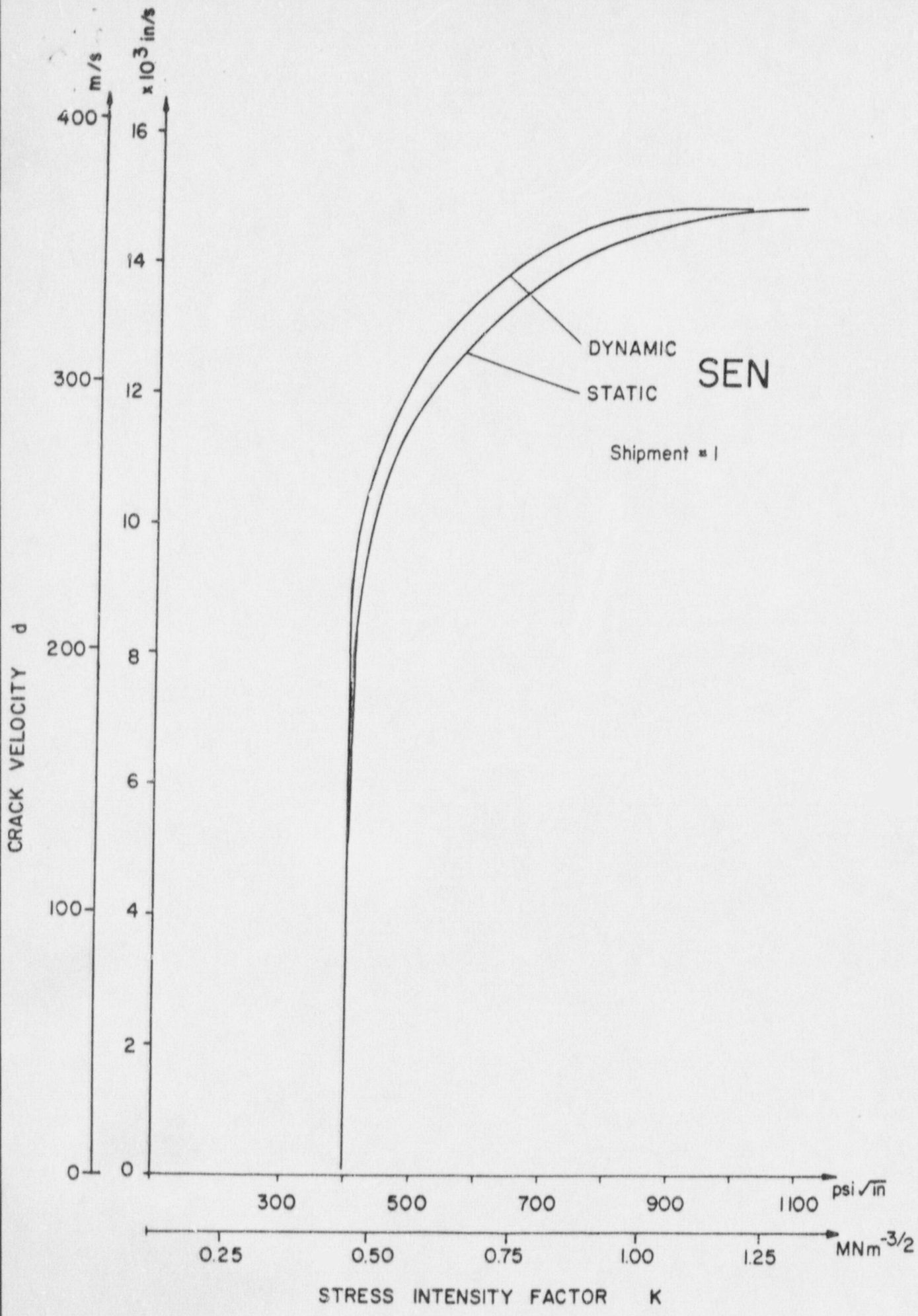
m/s
x10³ in/s
400
300
200
100
0
16
14
12
10
8
6
4
2
0
DYNAMIC
STATIC
SEN
Shipment # 1
CRACK VELOCITY d
300
500
700
900
1100
psi √in
0.25
0.50
0.75
1.00
1.25
MNm⁻³/²
STRESS INTENSITY FACTOR K

Fig 6

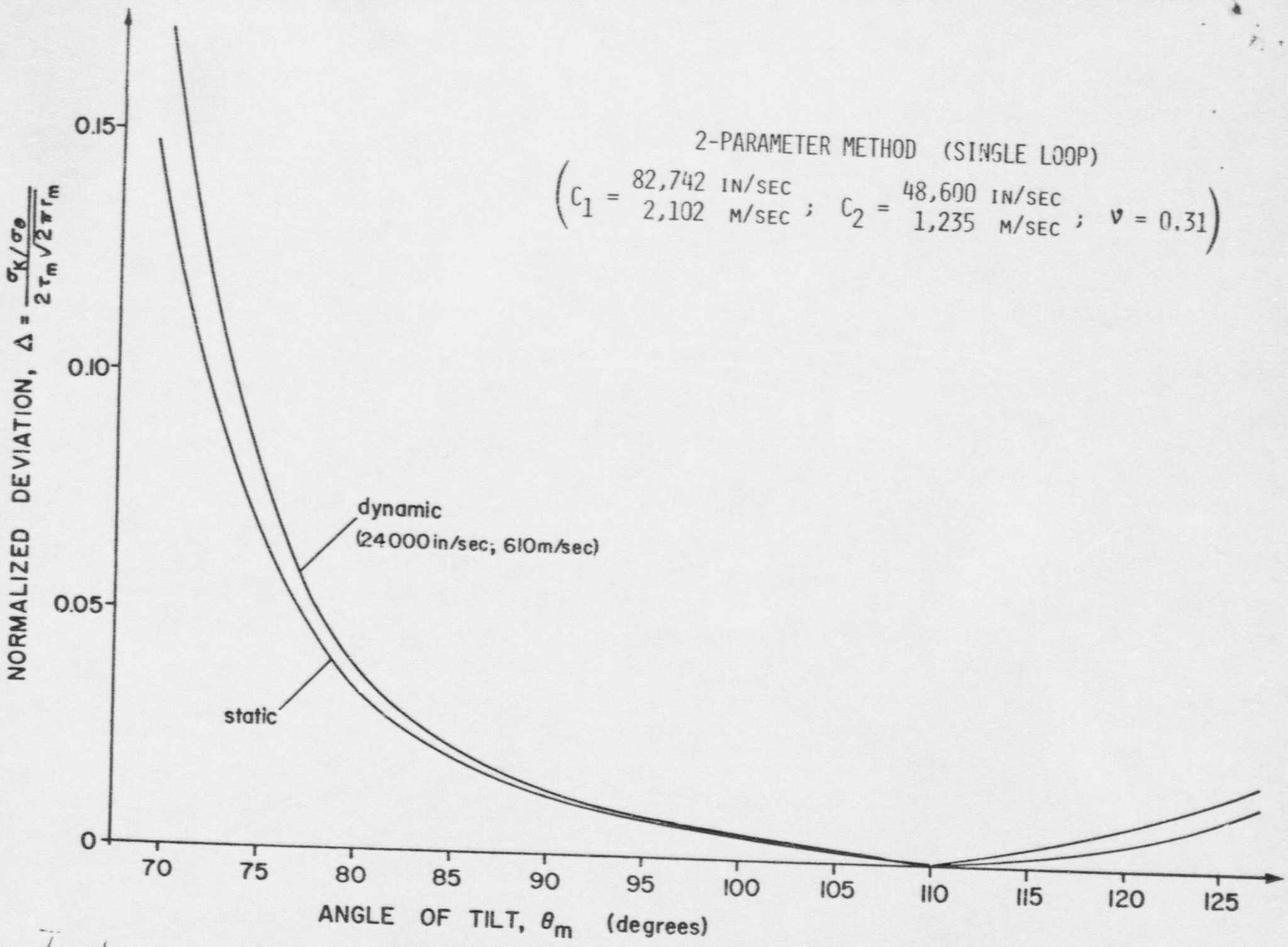
2-PARAMETER METHOD (SINGLE LOOP)
$C_1 = 82{,}742$ IN/SEC $= 2{,}102$ M/SEC ; $C_2 = 48{,}600$ IN/SEC $= 1{,}235$ M/SEC ; $\nu = 0.31$
NORMALIZED DEVIATION, $\Delta = \frac{\sigma_K/\sigma_\theta}{2\tau_m\sqrt{2\pi r_m}}$
0.15
0.10
0.05
0
dynamic
(24000 in/sec; 610m/sec)
static
70
75
80
85
90
95
100
105
110
115
120
125
ANGLE OF TILT, θ_m (degrees)